
The Eurasia Proceedings of Science, Technology, Engineering & Mathematics (EPSTEM)

Volume 1, Pages 178-186

ICONTES2017: International Conference on Technology, Engineering and Science

INFLUENCE OF Al CONTENT AND ASSOCIATED β -PHASE MORPHOLOGY ON CORROSION PROPERTIES OF Mg/Al ALLOYS

Sennur Candan
Bilecik Seyh Edebali University

Ercan Candan
Bilecik Seyh Edebali University

Abstract: The influence of the Al content and associated β morphology on the corrosion of Mg alloys has been studied using AZ41 and AZ91 series Mg alloys and compared with the corrosion of non Al containing Mg alloy (i.e AZ01). Scanning electron microscopy (SEM) was used for microstructural examinations. The corrosion behaviors were evaluated by immersion tests and potentiodynamic polarization measurements in 3.5% NaCl solution. The globular shaped β intermetallic phases were present in AZ41 alloy whereas they were transformed into a more coarsened lamellar or partially divorced β eutectics in AZ91 alloys. The results showed that the influence of Al addition on corrosion resistance was more pronounced up to 4 wt% (i.e AZ41) above which its influence was at less extent. The deterioration of the corrosion resistance of the alloys, at higher Al contents, was attributed to amount and morphology of β ($Mg_{17}Al_{12}$) intermetallics and the interruption of continuity of the oxide film on the surface of the alloys owing to coarsened β intermetallics.

Keywords: Mg alloy, AZ series alloys, casting, corrosion

Introduction

Magnesium-based alloys (AZ, AM, AS series) are increasingly used in many engineering areas including portable microelectronics, telecommunication, aerospace and automotive industries due to their low density (Friedrich and Mordike, 2006, Luo and Sachdev, 2012, Pekguleryuz, 2013, Manuel et al., 2015). Among the magnesium alloys, AZ series magnesium alloys are the most successfully used commercial alloys in these industries, which contains Al, Zn and a small quantity of Mn. However, the application of the AZ series magnesium alloys are still limited due to its limited strength and relatively lower corrosion resistance as compared to the aluminium alloys (Ghali, 2010). It is well known that formation of β -intermetallic ($Mg_{17}Al_{12}$) precipitates on the grain boundaries takes place in Mg alloys above 2 wt% Al content (Pekguleryuz, 2013, Cheng, 2009). The morphology of β intermetallic is mainly depended upon the the volume fraction of the Al content (Pardo et al., 2008, Candan and Candan, 2017), the solidification rate of the melt (Tanverdi, 2005, Candan et al., 2016) and minor alloying additions (Candan et al., 2009, Candan et al., 2011, Gusieva et al., 2015).

The number of the studies in the literature have been published on AZ series Mg alloys to understand their corrosion mechanisms (Cheng 2009, Pardo et al. 2008, Lunder et al.1989, Hehmann et al. 1987, Salman et al. 2010, Wang et al. 2012, Samaniego et el. 2013, Singh et al. 2015). However, the controversial views on the role of Al for the corrosion of AZ series magnesium alloy still exist. According to some researchers (Lunder et al.1989, Hehmann et al. 1987), the corrosion resistance of magnesium alloy improves in a noticeable level when aluminum content reaches 8-9% due to protective barrier effect of β -intermetallic promoted by Al content, while, some other researchers (Cheng 2009, Samaniego et el. 2013, Singh et al. 2015) reported that the β -intermetallics may not act as a protective barrier but may act as a micro-galvanic cells with the alloy matrix leading to a detrimental effect on corrosion resistance.

- This is an Open Access article distributed under the terms of the Creative Commons Attribution-Noncommercial 4.0 Unported License, permitting all non-commercial use, distribution, and reproduction in any medium, provided the original work is properly cited.

- Selection and peer-review under responsibility of the Organizing Committee of the conference

*Corresponding author: Sennur Candan- E-mail: sennur.candan@bilecik.edu.tr

Although, aforementioned studies (Pardo et al. 2008, Salman et al. 2010, Wang et al. 2012, Samaniego et al. 2013, Singh et al. 2015) above, dealt with corrosion behaviors of AZ series Mg alloys, these studies were carried out in a non-systematic manner. It is well known that alloying elements (Candan et al. 2009, Candan et al. 2011, Gusieva et al. 2015), cooling conditions (Tanverdi 2005, Candan et al. 2016) and production methods (i.e cast, rolled etc.) overwhelmingly affect the microstructure and, therefore, the corrosion resistance of the alloys. Therefore, the purpose of the present work is to gain a better understanding of the influence of Al content and associated β morphology by studying a comparative investigation on the corrosion behaviours of AZ41 and AZ91 alloys.

Methods

Master alloys were prepared by melting pure Mg together with pure Al in an electrical furnace under Ar gas atmosphere at 750 °C and cast as ingot form. The master alloy was then remelted and cast iron mold under protective SF₆ gas. The alloy specimens were used in as-cast form. AZ01 alloy, which contain no Al, was also prepared as control sample. The chemical compositions of the alloys, determined by Optical Emission Spectrometry (OES), are given in Table 1.

Table 1. Chemical composition of the AZ series magnesium alloys used (wt.%).

Alloys	Al	Mn	Zn	Fe	Mg
AZ01	0.4	0.28	1.22	0.002	Rest
AZ41	4.3	0.26	1.11	0.002	Rest
AZ91	9.5	0.21	0.84	0.002	Rest

Microstructural evaluations were carried out by scanning electron microscopy (SEM). Samples having 15mm in diameter and 10mm in length were machined and subsequently ground from 220 to 1200 grit emery papers followed by polishing with 1 μ m diamond paste for the immersion tests and microstructural evaluations. For SEM investigations, polished samples were etched in acetic-picral for a few seconds.

Two different immersion tests were employed: one was for mass loss measurements and the other was for observation of initial stage of the oxide film on the surface of the samples. For the mass loss measurements, the polished samples were weighed and then immersed in 3.5% NaCl solution for 72 h. After the immersion tests, the samples were cleaned with a solution containing 200 g/l CrO₃ for 15 min to remove the corrosion products. Finally, they were cleaned with distilled water, dried and weighed. The mass losses of the samples were then normalized in the unit of mg/cm² d by considering the total surface area of the samples. For the observation of the initial stage of the oxide film, the polished samples were immersed in 3.5% NaCl solution for 1/4 h then ultrasonically cleaned in distilled water and left to dry at room temperature.

For the potentiodynamic polarization measurements, machined samples of 9×9×9 mm were connected to copper wire and embedded in an epoxy resin holder. The surfaces were then abraded up to 1200 mesh emery paper, mechanically polished down to 1 μ m diamond paste and washed and ultrasonically rinsed in distilled water. The potentiodynamic curves were performed by means of a Gamry model PC4/300mA potentiostat/galvanostat controlled by a computer with DC105 mass analysis software. The embedded specimens in epoxy resin were utilized as working electrodes. A carbon rod (6 mm in diam.) and a saturated calomel electrode (SCE) were used as a counter electrode and reference electrode respectively. Experiments were performed at room temperature in a glass cell containing 3.5% NaCl solution. Each polarization experiment was carried out holding the electrode for 45 min. At open circuit potential (E_o) to allow steady-state to be achieved. Potentiodynamic polarization curves were generated by sweeping the potential from cathodic to anodic direction at a scan rate of 1 mVs⁻¹, starting from -2.00 up to 0.20 V. Each data point for both immersion and potentiodynamic polarization tests represents at least average of 3 different measurements.

Results and Findings

Microstructure

The microstructures of the examined AZ series Mg alloys are shown in Fig. 1(a-c). The microstructure consisted of primarily Mg-rich solid solution and secondary intermetallics both in the grain boundaries and occasionally within the α -Mg grains. The intermetallic phases had been increased with the increasing Al content (i.e AZ91)

and transformed to a coarsened net-like structure (Fig. 1c). High Magnification SEM micrograph is shown in Fig. 2. According to the Mg-Al equilibrium phase diagram, the eutectic β is expected to appear when the Al content reaches ~13 wt.%. However, the eutectic β intermetallic appears in alloys containing above 2 wt.% Al in nonequilibrium cooling conditions normally encountered in Mg alloy castings (Pekguleryuz 2013, Cheng 2009, Koc 2013). In higher Al containing alloys (i.e AZ91), lamellar and partially divorced β eutectics appear (Fig. 2). As reported previously (Candan et al. 2009, Candan et al. 2011, Boby et al. 2015), the eutectic with the lamellar structure in AZ91 Mg alloy is formed adjacent to the partially divorced eutectics in accord with the present work.

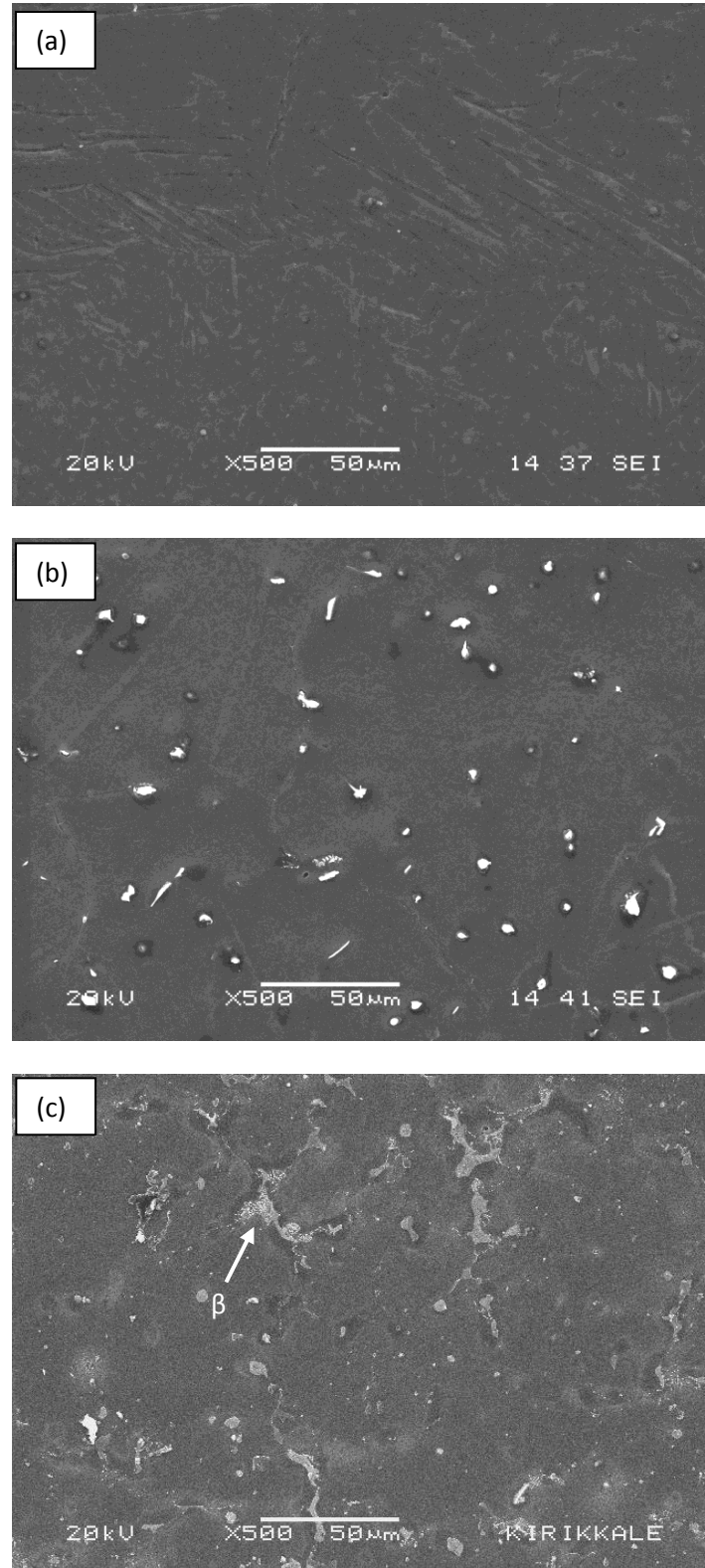


Figure 1. SEM Micrographs showing microstructure of (a) AZ01, (b) AZ41 and (c) AZ91 series Mg alloys.

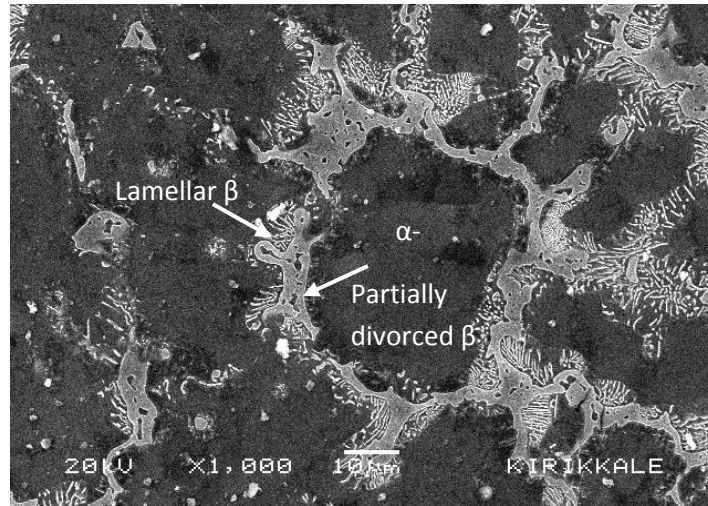


Figure 2. High magnification SEM morphology of the secondary intermetallics in AZ91 alloy

Corrosion

Figure 3 illustrates the results of mass loss from the immersion tests. Evidently, mass loss of the samples decreased immediately after addition of Al compared to non-Al containing alloy (i.e AZ01). However, the influence of Al addition was more pronounced up to 4 wt% (i.e AZ41) above which its influence was at less extent. Compared to AZ01 control alloy, the mass loss decreased nearly four fold in AZ41 alloy.

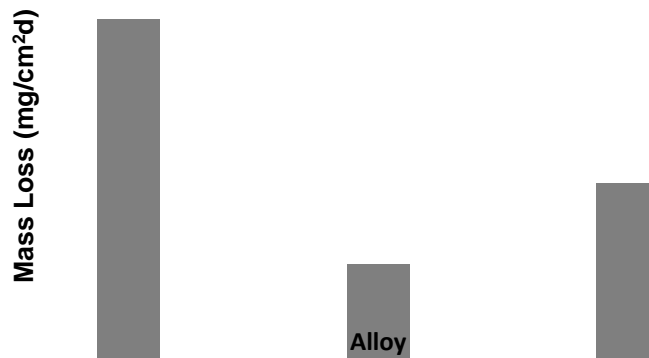


Figure 3. Mass loss of AZ series Mg alloys obtained from 72h immersion tests in 3.5% NaCl environment

Representative areas of the cross-sections immediately starting from the corroded surface to the inner part of the sample have been illustrated in the Fig. 4(a-c). The corrosion had propagated from the surface through inner part of the alloy, and many deep corrosion pits on the surface of the alloys took place. Evidently, AZ41 alloys exhibited much better corrosion resistance compared with AZ91 alloys indicating that the alloys containing higher Al contents (>4.0 wt.%), are subjected to a higher localized breakdown. The corrosion attack at the samples made of AZ91 alloy was tremendous that the corrosion, in some part of the samples, had been propagated through inner part of the AZ91 alloy by following the β intermetallic network as shown in Fig. 4(c).

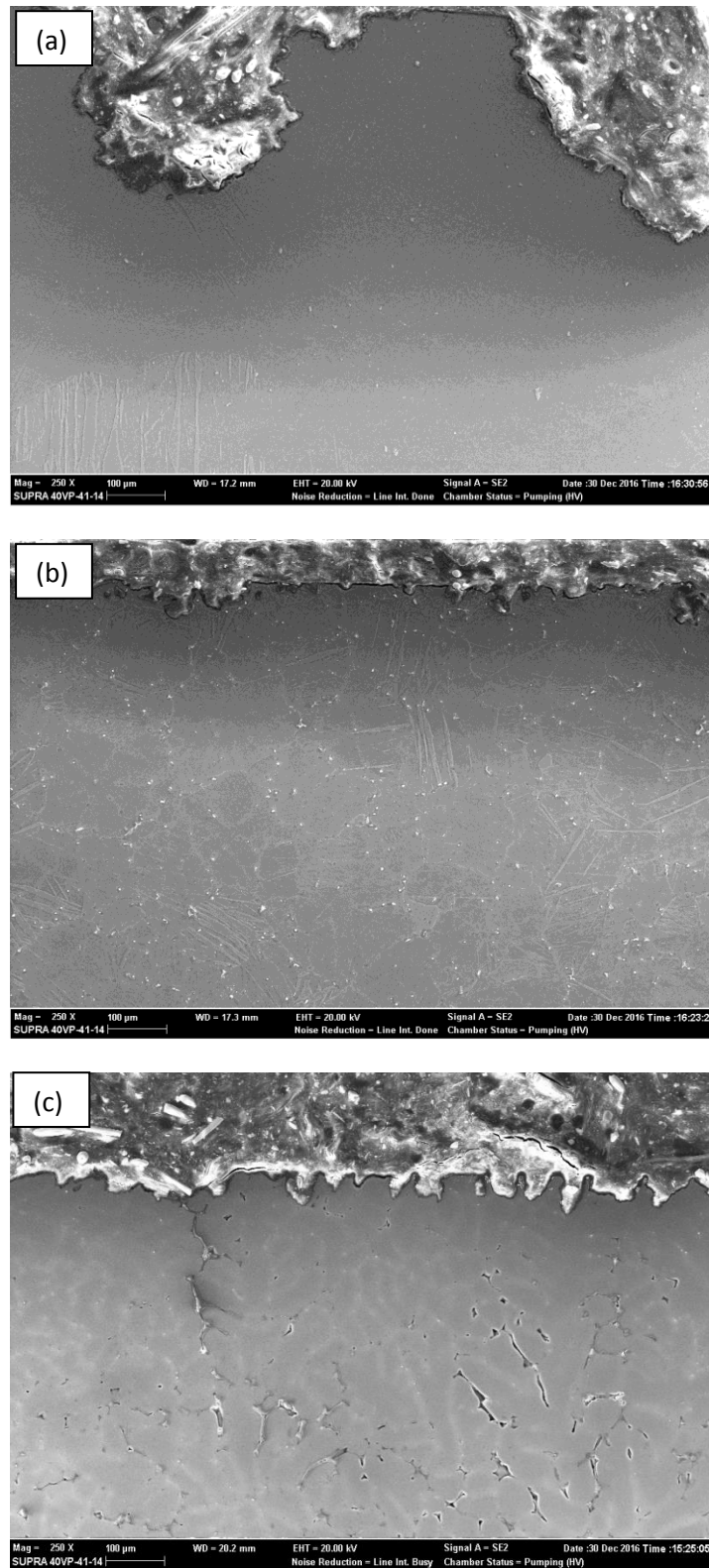


Figure 4. SEM micrographs showing cross section of (a) AZ01, (b) AZ41 and (c) AZ91 Mg alloys exposed to 3.5 wt.% NaCl for 72 h

Figure 5 shows potentiodynamic polarization curves of AZ01, AZ41 and AZ91 alloys. Their E_{corr} , I_{corr} values (obtained from Tafel-type fit technique) and calculated corrosion rates (CR) are summarised in Table 2. The corrosion rate (CR) conversions were carried out as suggested in Ref. (Cramer and Covino 1987) Compared to AZ01 control alloy, I_{corr} values of the AZ41 and AZ91 alloys decreased from 65.86 to 3.16 and 36 $\mu\text{A}/\text{cm}^2$ respectively. The results in Table 2 are very much in line with the mass loss results in Fig. 3.

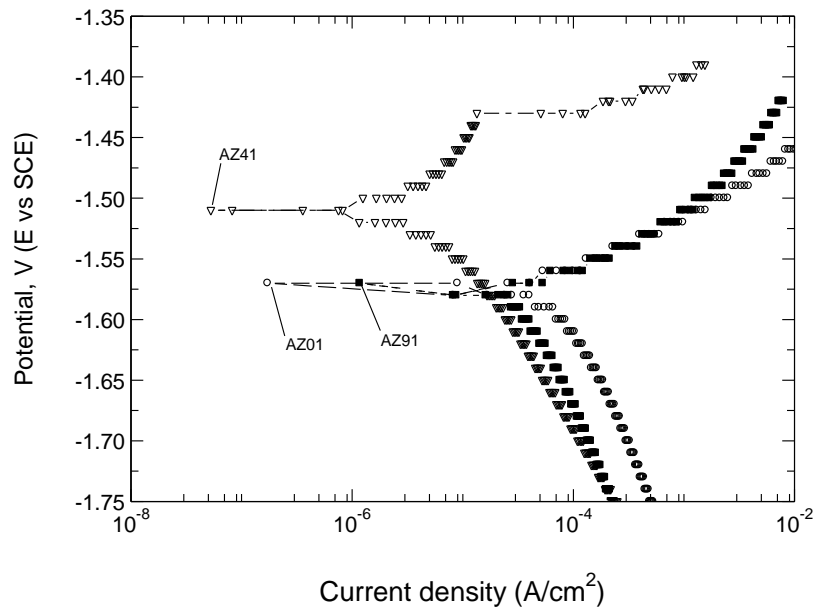


Figure 5. Potentiodynamic polarisation curves for AZ series Mg alloys in 3.5% NaCl environment.

 Table 2. E_{corr} , I_{corr} and CR values of AZ series Mg alloys derived from the polarization curves

Alloys	E_{corr} (mV/SCE)	I_{corr} ($\mu\text{A}/\text{cm}^2$)	CR (mm/y)
AZ01	-1571	65.86	1.51
AZ41	-1511	3.16	0.07
AZ91	-1573	36.0	0.82

Corrosion rate (mm/y) = 22.85 (current density mA/cm^2) (Cramer and Covino 1987)

Compared to AZ01 control alloy, better corrosion resistance of AZ41 and AZ91 alloys is attributed to Al content of Mg alloy. On the other hand, corrosion resistance of AZ41 alloy presented considerably better corrosion resistance than AZ91 alloy. As discussed earlier in the microstructure section, as Al content of the alloy increases, the presence of β intermetallic increases and its morphology coarsens. Based on galvanic corrosion principles, a higher amount of cathode (intermetallics) in relation to the size of the anode (α -Mg) results in an increased galvanic corrosion. Indeed, the highest mass loss is observed in AZ91 alloy since the ratio of the β intermetallics in AZ91 is higher than that of AZ41 alloys. Similar results have also been reported by (Samaniego et al. 2013, Singh et al. 2015) for AZ31 and AZ91 alloys. Contrarily, Refs. (Pardo et al. 2008, Salman et al. 2010) reported that corrosion resistance of AZ91 alloy was better than AZ31 alloy. They (Pardo et al. 2008, Salman et al. 2010) attributed these improvements to the barrier effect of β intermetallics. However, all of these works (Pardo et al. 2008, Salman et al. 2010) have been carried out by using electrochemical tests and not supported by long term immersion test (i.e. >24 h). It has been stated (Shi et al. 2010) that short-term corrosion tests to provide corrosion rates for Mg alloys do not agree with long-term tests. Often, the corrosion rate of Mg evaluated from Tafel extrapolation has pertained to conditions soon after specimen immersion and these corrosion rates have not related to steady state corrosion.

The addition of Al to Mg modifies the oxide film on the surface and the microstructure improving its resistance to the aggressive attack of Cl^- ions. Although, Al contents of AZ91 alloys are higher than that of AZ41 alloy, their higher mass loss may be due to discontinuity of the oxide film on the regions where relatively coarsened β intermetallics are present. The interruption of the continuity of the oxide film on the surface of the alloy, owing to formation of the coarsened intermetallics, is evident as shown in Fig. 6c. The hydration of the MgO occurs as exposed to water. The hydration of the MgO converts the cubic MgO to hexagonal $\text{Mg}(\text{OH})_2$ having a volume twice that of the oxide leading to a considerable disruption of the film and the formation of regions of charge instability (Liu et al. 2009). Propagation of the corrosion by following the intermetallic network in the microstructure is evident (Fig. 4c) attributed to disruption of the oxide film.

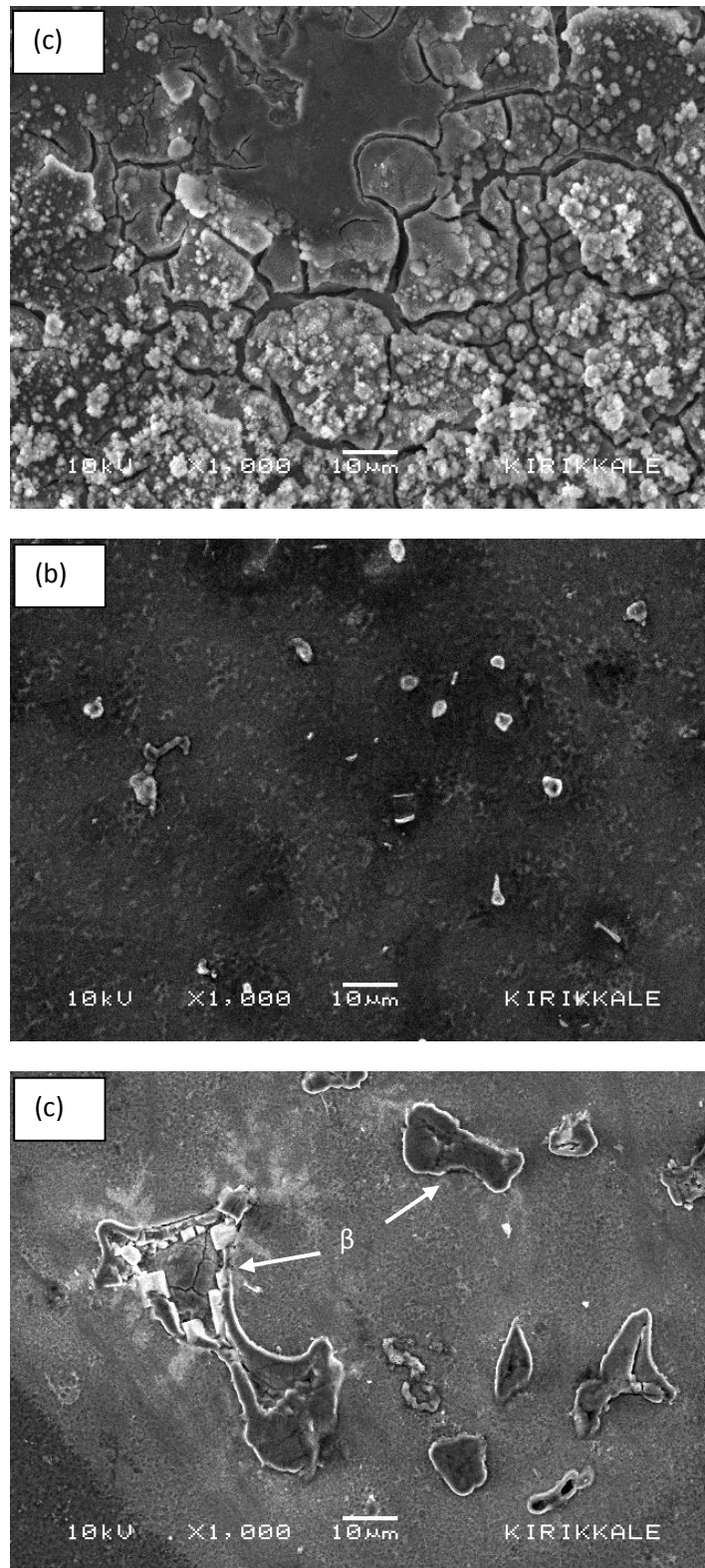


Figure 6. Surface morphologies showing the oxide film on the (a) AZ01, (b) AZ41 and (c) AZ91 alloys, exposed to 3.5% NaCl 1/4 h.

Conclusions

As Al content of the AZ series alloys increased (>4 wt.%), the globular shaped β intermetallic was transformed into a more coarsened lamellar or partially divorced β eutectics.

The results, from both the immersion tests and the potentiodynamic polarization measurements, showed that AZ41 alloy exhibited better corrosion resistance compared with the AZ91 alloy.

The corrosion attack at the samples made of AZ91 alloy is intense which is attributed to the influence of the morphology of β intermetallic and the disruption of the oxide film on the surface of the alloys.

References

- Boby, A., Srinivasan, A., Pillai, U. T. S., Pai, B. C. (2015). Mechanical characterization and corrosion behavior of newly designed Sn and Y added AZ91 alloy. *Materials and Design*, 88, 871-879.
- Candan, S., Unal, M., Koc, E., Turen, Y., Candan, E. (2011). Effects of titanium addition on mechanical and corrosion behaviours of AZ91 magnesium alloy. *Journal of Alloys and Compounds*, 509, 1958-1963.
- Candan, S., & Candan, E. (2017). A Comparative study on corrosion of Mg-Al-Si alloys. *Transactions of Nonferrous Metals Society of China*, (In press).
- Candan, S., Celik, M., Candan, E. (2016). Effectiveness of Ti-micro alloying in relation to cooling rate on corrosion of AZ91 Mg Alloy. *Journal of Alloys and Compounds*, 672, 197-203.
- Candan, S., Unal, M., Turkmen, M., Koc, E., Turen Y., Candan, E. (2009). Improvement of mechanical and corrosion properties of magnesium alloy by lead addition. *Materials Science and Engineering A*, 501, 115-118.
- Cheng, Ying-Liang, Qin, Ting-Wei, Wang, Hui-Min, Zhang, Zhao. (2009). Comparison of corrosion behaviors of AZ31, AZ91, AM60 and ZK60 magnesium. *Transactions of Nonferrous Metals Society of China*, 19, 517-524.
- Cramer, S.D., & Covino, B.S., Jr (Eds). (1987). *ASM International, Corrosion, Metals Handbook*, Materials Park, Ohio, OH: The Materials International Society.
- Friedrich, H. E., & Mordike, B. L. (2006). *Magnesium technology metallurgy, design data, applications*. 1st ed. Berlin: Springer-Verlag.
- Ghali, E., (2010). *Corrosion resistance of aluminum and magnesium alloys, understanding, performance and testing*. 1st ed. New Jersey: Wiley Publishing.
- Gusieva, K., Davies, C. H. J., Scully, J. R., Birbilis, N. (2015). Corrosion of magnesium alloys: the role of alloying. *International Materials Reviews*, 60, 169-194.
- Hehmann, F., Froes, F. H., Young, W. (1987). Rapid solidification of aluminium, magnesium and titanium. *Journal of Metals*, 39(8), 14-21.
- Koc, E. (2013). An investigation on corrosion dependent mechanical behaviours of biodegradable magnesium alloys. Karabuk University, Institute of Science and Technology.
- Liu, M., Zanna, S., Ardelean, H., Frateur, I., Schmutz, P., Song, G.L., Atrens, A., Marcus, P. (2009). A first quantitative XPS study of the surface films formed, by exposure to water, on Mg and on the Mg-Al intermetallics: Al_3Mg_2 and $\text{Mg}_{17}\text{Al}_{12}$. *Corrosion Science*, 51, 1115-1127.
- Lunder, O., Lein, J. E., Aune, T. K., Nisancioğlu, K. (1989). The role of magnesium aluminium ($\text{Mg}_{17}\text{Al}_{12}$) phase in the corrosion of magnesium alloy AZ91. *Corrosion*, 45, 741-748.
- Luo, A. A., & Sachdev, A. K. (2012). *Applications of magnesium alloys in automotive engineering*, C. Bettles, M. Barnett, Wrought Magnesium Alloys (pp. 393-426). Woodhead Publishing.
- Manuel, M. V., Singh, A., Alderman, M., Neelameggham N., (2015). *Magnesium technology*, M.V. Manuel, A. Singh, M. Alderman, N.R. Neelameggham. Wiley-TMS Publishing.
- Pardo, A., Merino, M. C., Coy, A. E., Viejo, F., Arrabal, R., Feliú, S. Jr. (2008). Influence of microstructure and composition on the corrosion behaviour of Mg/Al alloys in chloride media. *Electrochimica Acta*, 53, 7890-7902.
- Pekguleryuz, M., (2013). Alloying behavior of magnesium and alloy design, M.O. Pekguleryuz, K.U. Kainer, A.A. Kaya. *Fundamentals of Magnesium Alloy Metallurgy* (pp. 152-196). Woodhead Publishing.
- Salman, S. A., Ichino, R., Okido, M. (2010). A Comparative electrochemical study of AZ31 and AZ91 magnesium alloy. *International Journal of Corrosion*, 1-7.
- Samaniego, A., Llorente, I., Feliu, Jr S. (2013). Combined effect of composition and surface condition on corrosion behaviour of magnesium alloys AZ31 and AZ61. *Corrosion Science*, 68, 66-71.
- Shi, Z., Liu, M., Atrens, A. (2010). Measurement of the corrosion rate of magnesium alloys using tafel extrapolation. *Corrosion Science*, 52, 579-588.
- Singh, I. B., Singh, M., Das, S. (2015). A comparative corrosion behavior of Mg, AZ31 and AZ91 alloys in 3.5% NaCl solution. *Journal of Magnesium and Alloys*, 3, 142-148.

- Tanverdi, A. (2005). *Effect of solidification rate and Si and Y additions on corrosion behavior of AZ91 Mg alloy*. Eskisehir: Osmangazi University, Institute of Science and Technology.
- Wang, Lei., Shinohara, T., Zhang, Bo-Ping. (2012). Electrochemical behaviour of AZ61 magnesium alloy in dilute NaCl solutions. *Materials and Design*, 33, 345-349.